Determination of the Rate-Limiting Step in the Hepatic Elimination of YM796 by Isolated Rat Hepatocytes

Takafumi Iwatsubo,[1] Hiroshi Suzuki,[2] and Yuichi Sugiyama[2,3]

Received August 19, 1998; accepted October 13, 1998

Purpose. The membrane permeability clearance and intrinsic metabolic clearance of a drug in the liver were estimated using isolated rat hepatocytes, and the rate-limiting step in the overall intrinsic clearance of the drug *in vivo* was investigated. For this purpose, an anti-dementia drug, (S)-(-)-2,8-dimethyl-3-methylene-1-oxa-8-azaspiro [4,5] decane-L-tartarate monohydrate (YM796) was used as a model drug.

Methods. The parent drug and its metabolites in both medium and cells were separated by thin-layer chromatography (TLC). The total amount of drug taken up by hepatocytes and the total amount of metabolites were plotted against the AUC of YM796 in the medium or cells to obtain the kinetic parameters.

Results. While the influx clearance (PS_{inf}) through the sinusoidal membrane defined in terms of YM796 concentration in the medium was almost constant, irrespective of the concentration of YM796 in the medium, the intrinsic metabolic clearance (CL_{int}) and the efflux clearance (PS_{eff}) defined in terms of the total concentration of YM796 in the cells markedly decreased and increased, respectively, as the concentration of YM796 increased. The overall intrinsic metabolic clearance ($CL_{int,all}$), defined in terms of the YM796 concentration in the medium, corresponding to the hepatic intrinsic clearance obtained from the *in vivo* pharmacokinetic data on the drug, was comparable with PS_{inf} at low concentrations of YM796. As the YM796 concentration increased, however, $CL_{int,all}$ fell markedly approaching CL_{int}.

Conclusions. While, at low concentrations of YM796, $CL_{int,all}$ was predominantly affected by membrane permeability clearance, at high concentrations it was completely rate-determined by the intrinsic metabolic clearance because of the marked reduction in CL_{int} resulting from the saturation of YM796 metabolism.

KEY WORDS: clearance; efflux; hepatocytes; influx; membrane permeability; metabolism; rate-limiting step.

INTRODUCTION

(S)-(-)-2,8-dimethyl-3-methylene-1-oxa-8-azaspiro [4,5] decane-L-tartarate monohydrate (YM796) is a selective M1-receptor agonist and is currently being developed for the treatment of dementia. We previously reported that YM796 was eliminated from the body mainly by hepatic metabolism seen in rats, dogs, and humans, and the *in vivo* pharmacokinetics of the drug following oral administration could be accurately predicted from *in vitro* metabolism data (1,2). Furthermore, for many other drugs which are metabolized by P-450, a good correlation was observed between the intrinsic metabolic clearances obtained from the *in vitro* studies ($CL_{int,in\ vitro}$) and those calculated from their *in vivo* pharmacokinetic data ($CL_{int,in\ vivo}$) (3,4). However, in calculating the $CL_{int,in\ vivo}$ values, it was assumed that the unbound concentration of drug in the liver rapidly became equilibrated with that in blood (the assumption of rapid equilibrium between blood and hepatocytes), and that there was no active transport of the drug. These assumptions are not always true and, for some drugs, it is suggested that $CL_{int,in\ vivo}$ depends not only upon the hepatic metabolic clearance but also upon the permeability clearance through the sinusoidal membrane (5,6).

In the present study, using YM796 as a model drug, the concentration-dependence of the membrane permeability clearance and the intrinsic metabolic clearance were investigated with isolated rat hepatocytes, and the rate-limiting step in the disappearance of the drug from plasma is discussed.

MATERIALS AND METHODS

Chemicals and Reagents

YM796 and [^{14}C-]YM796 were synthesized by Yamanouchi Pharmaceutical Co., Ltd (Tokyo, Japan) and by Amersham International (Buckinghamshire, UK), respectively. N-2-hydroxyethylpiperazine-N'-2-ethanesulfonic acid (HEPES), Methanol, and chloroform were purchased from Wako Pure Chemical Industries, Ltd (Osaka, Japan). All other chemicals were of reagent grade.

Cell Preparation

Hepatocytes were prepared from male Wistar rats (250–320 g) by the procedure of Baur *et al.* (7). Hepatocytes were suspended (approximately 2 mg protein/ml) at 0°C in albumin-free Krebs-Henseleit buffer supplemented with 12.5 mM HEPES (pH 7.4) after isolation. Cell viability of the hepatocytes used in this study was routinely checked by the trypan blue [0.4% (wt/vol)] exclusion test, being 91% in average.

[1] Drug Metabolism Laboratories, Yamanouchi Pharmaceutical Co., Ltd., 1-1-8, Azusawa, Itabashi-ku, Tokyo 174, Japan.

[2] Faculty of Pharmaceutical Sciences, The University of Tokyo, 7-3-1, Hongo, Bunkyo-ku, Tokyo 113, Japan.

[3] To whom correspondence should be addressed. (e-mail: bxg05433@nifty.ne.jp)

ABBREVIATIONS: AUC, Area under the concentration-time curve; AUC_{cell}, Area under the concentration-time curve for intact drug in the cells; AUC_{med}, Area under the concentration-time curve for intact drug in the medium; C_{cell}, Total concentration of intact drug in the cells; $C_{cell,ss}$, Total concentration of intact drug in the cells at steady-state; C_{med}, Intact drug concentration in the medium; $C_{med,ss}$, Intact drug concentration in the medium at steady-state; CL_{int}, Intrinsic metabolic clearance defined in terms of the total concentration of intact drug in the cells; $CL_{int,all}$, Overall intrinsic metabolic clearance defined in terms of the intact drug concentration in the medium; $CL_{int,in\ vitro}$, Intrinsic metabolic clearance obtained from the *in vitro* studies; $CL_{int,in\ vivo}$, Intrinsic metabolic clearance calculated from the *in vivo* pharmacokinetic data; $CL_{u,int}$, Intrinsic clearance for hepatic metabolism defined in terms of the unbound drug; f_T, Unbound fraction in the cells; $K_{m,app}$, Apparent Michaelis constant; PS_{eff}, Efflux clearance through the sinusoidal membrane defined in terms of the total concentration of intact drug in the cells; PS_{inf}, Influx clearance through the sinusoidal membrane defined in terms of intact drug concentration in the medium; $PS_{u,eff}$, Membrane permeability clearance for efflux defined in terms of the unbound drug; $PS_{u,inf}$, Membrane permeability clearance for influx defined in terms of the unbound drug; TLC, Thin-layer chromatography; V_{max}, Maximum metabolic rate; $X_{m(cell+med)}$, Sum of the amounts of total metabolites both in the medium and cells; $X_{p,cell}$, Amount of intact drug in the cells; X_t Sum of the amounts of intact drug in the cells and total metabolites both in the medium and cells.

0724-8741/99/0100-0110$16.00/0

Uptake Study

Uptake of [^{14}C-]YM796 was initiated by adding the ligand to the preincubated (at 37°C for 3 min) cell suspension. The reaction was terminated at designated times by separating the cells from the medium by centrifugal filtration (8). The intact [^{14}C-]-YM796, both in the medium and in cells, was separated from the metabolites as follows: Aliquots of the hepatocyte incubation mixture containing [^{14}C-]YM796 were layered on a mixture of silicon and mineral oil (density 1.015) contained in a microfuge tube. After centrifugation, 150 μl of the medium layer was removed and added to 300 μl of methanol. After the residual medium layer and the oil mixture were removed, the whole cell pellet was added to methanol to precipitate proteins. Aliquots of both the medium and cell extracts were applied to a TLC plate (Kiesel gel 60 F254, Merck, FRG), and the quantitation of both intact [^{14}C-]YM796 and metabolites was performed using BAS-2000 equipment (Fuji-film, Tokyo, Japan) as described previously (1). The cellular uptake rates of YM796 were corrected for the adherent fluid volume (2.1 μl) and then converted to intracellular concentrations by taking into consideration the intracellular space (4.3 μl), as reported previously (9).

Data Analysis

The rate of metabolism for YM796 by hepatocytes can be described by the following differential equation

$$dX_{m(cell+med)}/dt = CL_{int,all} \cdot C_{med} \quad (1)$$

where $X_{m(cell+med)}$ [nmol/mg protein] is the sum of the amounts of total metabolites both in the medium and in cells, and $CL_{int,all}$ [μl medium/min/mg protein] is the overall intrinsic metabolic clearance defined against the intact YM796 in the medium (C_{med} [nmol/μl medium]) which corresponds to the *in vivo* intrinsic clearance calculated from the plasma concentration data. Integration of Eq. (1) gives

$$X_{m(cell+med)}(t) = CL_{int,all} \cdot AUC_{med}(0\text{-}t) \quad (2)$$

where $AUC_{med}(0\text{-}t)$ [nmol · min/μl medium] represents the area under the concentration-time curve from time 0 to t for YM796 in the medium. The $CL_{int,all}$ value can be obtained from the slope of a plot of $X_{m(cell+med)}(t)/C_{med}(0)$ vs. $AUC_{med}(0\text{-}t)/C_{med}(0)$ designated as the integration plot (9).

Then, the following equation was used for the fitting analysis of the metabolism data sets by an iterative nonlinear least squares method using MULTI (10) to obtain the apparent Michaelis constant ($K_{m,app}$ [μM]) and the maximum metabolic rate (V_{max} [nmol/min/mg protein]) for YM796 metabolism.

$$CL_{int,all} = V_{max}/(K_{m,app} + C_{med}) \quad (3)$$

The rate of metabolism of YM796 by hepatocytes can also be described by the following differential equation

$$dX_{m(cell+med)}/dt = CL_{int} \cdot C_{cell} \quad (4)$$

where CL_{int} [μl cellular space/min/mg protein] is the intrinsic metabolic clearance defined against the total concentration of intact YM796 in the cells (C_{cell} [nmol/μl cellular space]). On the other hand, the mass-balance of intact YM796 in the cells

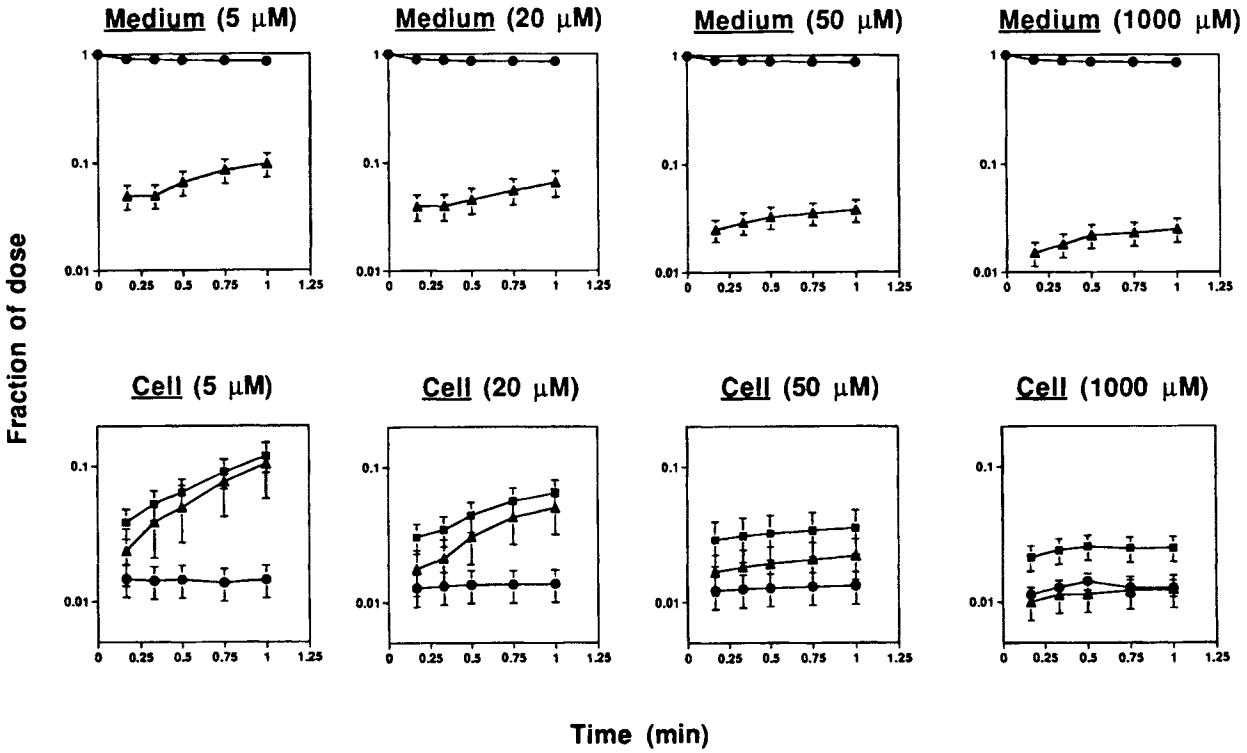

Fig. 1. Time-course of uptake and metabolism of YM796 by isolated rat hepatocytes at various concentrations (5, 20, 50 and 1000 μM) of YM796. Both intact YM796 and metabolites were determined using BAS-2000 equipment (Fuji-film, Tokyo, Japan) as described previously (1), and the results are shown as a fraction of the dose. ●, parent (YM796), ▲, metabolites, ■, total drugs (sum of parent and metabolites).

can be described by the following differential equation

$$dX_{p,cell}/dt = PS_{inf} \cdot C_{med} - (PS_{eff} + CL_{int}) \cdot C_{cell} \quad (5)$$

where $X_{p,cell}$ [nmol/mg protein] is the amount of intact YM796 in the cells, PS_{inf} [μl medium/min/mg protein] is the influx clearance defined against C_{med}, and PS_{eff} [μl cellular space/min/mg protein] is the efflux clearance defined against C_{cell}, respectively. The sum of equations (4) and (5) gives equation (6).

$$dX_t/dt = PS_{inf} \cdot C_{med} - PS_{eff} \cdot C_{cell} \quad (6)$$

where X_t (nmol/mg protein) is the sum of $X_{p,cell}$ and $X_{m(cell+med)}$. Integration of Eq. (6) gives

$$X_t(t) = PS_{inf} \cdot AUC_{med}(0\text{-}t) - PS_{eff} \cdot AUC_{cell}(0\text{-}t) \quad (7)$$

where $AUC_{cell}(0\text{-}t)$ [nmol · min/μl cellular space] represents the area under the concentration-time curve from time 0 to t for YM796 in the cells. The PS_{inf} value can be obtained from the initial slope of a plot of $X_t(t)/C_{med}(0)$ vs. $AUC_{med}(0\text{-}t)/C_{med}(0)$ during the very early period when the efflux of intact YM796 is negligible.

In addition, integration of Eq. (4) gives

$$X_{m(cell+med)}(t) = CL_{int} \cdot AUC_{cell}(0\text{-}t) \quad (8)$$

Thus, the CL_{int} value can be obtained from the slope of a plot of $X_{m(cell+med)}(t) / C_{med}(0)$ vs. $AUC_{cell}(0\text{-}t)/C_{med}(0)$.

At steady-state, Eq. (9) can be obtained from Eq. (5). The cell-to-medium concentration ratio at steady-state ($C_{cell,ss}/C_{med,ss}$) is described as a function of PS_{inf}, PS_{eff} and CL_{int} as described below.

$$C_{cell,ss}/C_{med,ss} = PS_{inf}/(PS_{eff} + CL_{int}) \quad (9)$$

The PS_{eff} can be obtained from the PS_{inf} and CL_{int} values estimated from Eqs. (7) and (8) together with the cell-to-medium concentration ratio data at steady-state.

Furthermore, $CL_{int,all}$ can also be expressed as a hybrid parameter for PS_{inf}, PS_{eff} and CL_{int} based on Eqs.(1), (4) and (9) as described below.

$$CL_{int,all} = PS_{inf} \cdot CL_{int}/(PS_{eff} + CL_{int}) \quad (10)$$

The tissue binding of YM796 was also estimated as follows. Under conditions where no metabolism of YM796 occurs ($CL_{int} = 0$), Eq. (9) gives

$$C_{cell,ss}/C_{med,ss} = PS_{inf}/PS_{eff} = 1/f_T \quad (11)$$

where f_T represents the unbound fraction of YM796 in the cells. The cell-to-medium concentration ratio at steady-state was measured to estimate the f_T value under the following three experimental conditions where no metabolism of YM796 is assumed to occur; (i)in the presence of SKF-525A (500 μM) which is a typical inhibitor of P-450, (ii) at low temperature (4°C), and (iii) after treatment with carbon monoxide (CO) which also inhibits P-450 activity.

RESULTS

Time-Course of the Fraction of the Dose Represented by Intact YM796 and Total Metabolites in the Medium and Cells

The time-courses of the proportion of dose represented by intact YM796 and total metabolites in the medium and cells at the initial YM796 concentrations of 5, 20, 50 and 1000 μM are shown in Figure 1. At 1 min after incubation, the proportion of metabolites to the total amount of drug in the cells was 87% at 5 μM, and this fell as the concentration of YM796 increased, finally reaching approximately 50% at 1000 μM. The proportion of metabolites in terms of the dose also fell from 9.8% to 2.5% as the concentration of YM796 increased from 5 to 1000 μM.

Concentration-Dependence of $CL_{int,all}$

In Figure 2, the total amount of metabolites normalized by the initial YM796 concentrations (5 ~ 1000 μM) in the medium were plotted against the AUC of YM796 in the medium normalized by the initial YM796 concentrations. $CL_{int,all}$ estimated from the initial slope of the plots based on Eq. (2) fell markedly from 112 to 1.5 μl medium/min/mg protein as the initial concentration of YM796 in the medium increased from 5 to 1000 μM (Fig. 3(A)). The Eadie-Hofstee plots for YM796 metabolism are shown in Figure 3(B). By fitting analysis of the metabolism data based on Eq. (3), $K_{m,app}$ and V_{max} were calculated to be 18.6 μM and 2.06 nmol/min/mg protein, respectively.

Concentration-Dependence of PS_{inf}

The total amount of drug taken up by hepatocytes normalized by the initial YM796 concentrations (5 ~ 1000 μM) in the medium were plotted against the AUC of YM796 in the medium normalized by the initial YM796 concentrations in Figure 4. PS_{inf} estimated from the initial slope of the plots based on Eq. (7) was relatively constant ranging from 114 to 93 μl medium/min/mg protein over initial YM796 concentrations ranging from 5 to 1000 μM (Fig. 5).

Concentration-Dependence of CL_{int}

In Figure 6, the total amount of metabolites normalized by the initial YM796 concentrations (5 ~ 1000 μM) in the

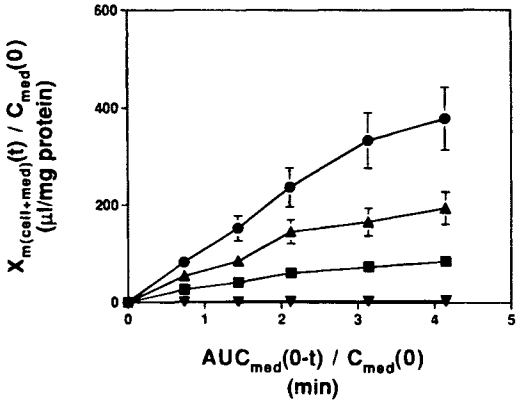

Fig. 2. Integration plots for the total amount of YM796 metabolites against the area under the concentration-time curve for intact YM796 in the medium. The sum of the amount of total metabolites in both cells and medium were plotted against the area under the concentration-time curve for intact YM796 in the medium, and both ordinate and abscissa were normalized by the initial concentration of YM796 in the medium. The $CL_{int,all}$ values were obtained from the initial slope of the plots based on Eq. (2). ●, 5 μM, ▲, 20 μM, ■, 50 μM, ▼, 1000 μM.

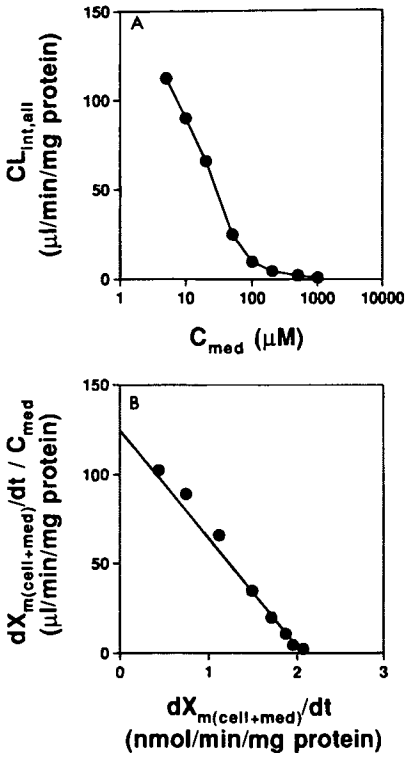

Fig. 3. Concentration-dependence of $CL_{int,all}$ (A) and Eadie-Hofstee plots for YM796 metabolite formation (B). The $CL_{int,all}$ values were estimated from Eq. (2) at each concentration of YM796 used (5 ~ 1000 μM). Eq. (3) was fitted to the YM796 metabolism data sets to obtain the $K_{m,app}$ and V_{max} values. The $K_{m,app}$ and V_{max} were estimated to be 18.6 μM and 2.06 nmol/min/mg protein, respectively.

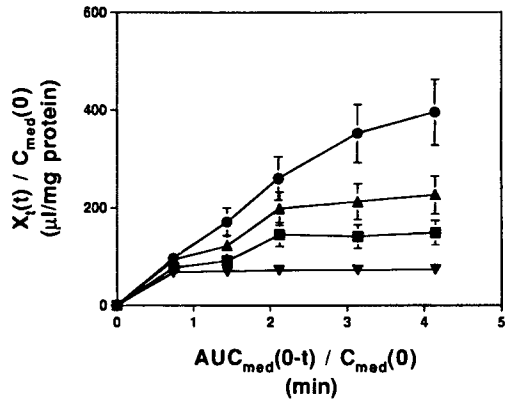

Fig. 4. Integration plots for the uptake of YM796 against the area under the concentration-time curve for intact YM796 in the medium. The sum of the amount of both YM796 and total metabolites in the cells and the amount of total metabolites in the medium were plotted against the area under the concentration-time curve for intact YM796 in the medium, and both ordinate and abscissa were normalized by the initial concentration of YM796 in the medium. The PS_{inf} values were obtained from the initial slope of the plots based on Eq. (7). ●, 5 μM, ▲, 20 μM, ■, 50 μM, ▼, 1000 μM.

medium were plotted against the AUC of YM796 in the cells normalized by the initial YM796 concentrations. CL_{int} estimated from the initial slope of the plots based on Eq. (8) fell markedly from 102 to 1.5 μl cellular space/min/mg protein as the initial YM796 concentration increased from 5 to 1000 μM (Fig. 5).

Concentration-Dependence of PS_{eff}

PS_{eff} was calculated to be 26 μl cellular space/min/mg protein at 5 μM YM796 from the PS_{inf} and CL_{int} values estimated above based on Eq. (9) and increased as the concentration of YM796 increased, finally reaching 91 μl cellular space/min/mg protein, at 1000 μM, which was almost comparable with PS_{inf} (Fig. 5).

Tissue Binding

The time-courses of the cell-to-medium concentration ratio at 5 and 1000 μM YM796 under three conditions, (A) in the presence of SKF-525A (500 μM), (B) at low temperature (4°C), and (C) following treatment with CO, are shown in Figure 7. The cell-to-medium concentration ratio had almost reached steady-state within 5 min after the initiation of incubation, and the f_T values calculated based on Eq. (11) were almost comparable under all conditions being 0.40 ~ 0.42 at 5 μM and 0.83 ~ 0.98 at 1000 μM, suggesting that there was a reduction in the tissue binding of YM796 when the concentration of YM796 increased.

DISCUSSION

We previously reported that YM796 was eliminated from the body mainly by hepatic metabolism seen in rats, dogs, and humans, and that the $CL_{int,in\ vitro}$ values obtained from the *in vitro* metabolism studies using liver microsomes prepared from each species were relatively similar to the $CL_{int,in\ vivo}$ ($CL_{int,all}$) values calculated using the dispersion model from the *in vivo* pharmacokinetic data after oral administration of the drug (1,2). $CL_{int,all}$ is a hybrid parameter as shown by Eq. (12), and affected not only by $CL_{u,int}$ which represents the intrinsic clearance for hepatic metabolism but also by $PS_{u,inf}$ and $PS_{u,eff}$ which are defined as the membrane permeability clearance for influx and efflux in terms of the unbound drug, respectively.

$$CL_{int,all} = PS_{u,inf} \times CL_{u,int}/(PS_{u,eff} + CL_{u,int}) \quad (12)$$

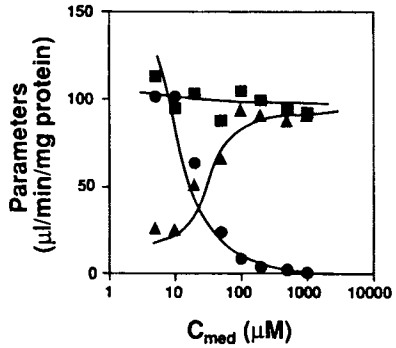

Fig. 5. Concentration-dependence of PS_{inf}, PS_{eff} and CL_{int}. The PS_{inf}, PS_{eff} and CL_{int} values were estimated from Eqs. (7), (9) and (8), respectively, at each YM796 concentration used (5 ~ 1000 μM). ■, PS_{inf}, ▲ PS_{eff}, ●, CL_{int}.

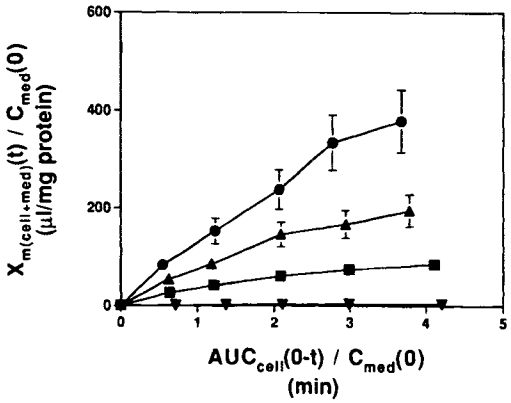

Fig. 6. Integration plots for total amount of YM796 metabolites against the area under the concentration-time curve for intact YM796 in the cells. The sum of the amount of total metabolites in both cells and medium were plotted against the area under the concentration-time curve for intact YM796 in the cells, and both ordinate and abscissa were normalized by the initial YM796 concentration in the medium. The CL_{int} values were obtained from the initial slope of the plots based on Eq. (8). ●, 5 μM, ▲, 20 μM, ■, 50 μM, ▼, 1000 μM.

Eq. (12) clearly shows that $CL_{int,all}$ becomes equal to $CL_{u,int}$ only when $PS_{u,eff}$ is equal to $PS_{u,inf}$ and is much greater than $CL_{u,int}$. However, these assumption are not always true. For instance, *l*-propranolol has been demonstrated to show a concentration-dependent shift in the rate-determining process of its overall intrinsic hepatic clearance, which is a combination of membrane permeability and sequestration at low concentrations, whereas at high concentrations, the rate-determining process is sequestration (11). Pravastatin, a HMG-CoA reductase inhibitor, has also been demonstrated to be taken up into the liver by a carrier-mediated active transport system, and the uptake by this system is the rate-limiting step in the overall intrinsic hepatic clearance of the drug (12). Thus, in the present study, to examine whether the previously mentioned condition is true for YM796, we have quantitatively estimated both the membrane permeability clearance and the intrinsic metabolic clearance for YM796 using isolated rat hepatocytes.

$CL_{int,all}$ which is a hybrid parameter of influx, efflux, and intrinsic metabolic clearances, and directly corresponds to $CL_{int,in\ vivo}$ calculated from the *in vivo* pharmacokinetic data on the drug, fell as the concentration of YM796 increased, showing marked nonlinearity (Fig. 3(A)). As shown in Figure 3(B), YM796 metabolism by rat hepatocytes was represented as a single component reaction and considered to reflect the same metabolic reaction observed in liver microsomes reported previously (2). The $K_{m,app}$ and V_{max} values obtained by fitting analysis based on Eq. (3) were 18.6 μM and 2.06 nmol/min/mg protein, respectively. The $K_{m,app}$ value was comparable with that obtained in rat liver microsomes (13.4 μM) (2). The V_{max} value was converted to 542 nmol/min/g liver taking into consideration the protein content in the cells (2.1 mg protein/10^6 cells) used in the present study and the number of the cells per one gram of liver (1.25×10^8 cells/g liver) (13). This is also similar to what was obtained in liver microsomes (520 nmol/min/g liver) previously described (2). Furthermore, the overall intrinsic hepatic clearance under linear conditions calculated from these parameters ($CL_{int,all} = V_{max}/K_{m,app}$) was 29.1 ml/min/g liver, which was slightly low, but relatively comparable with

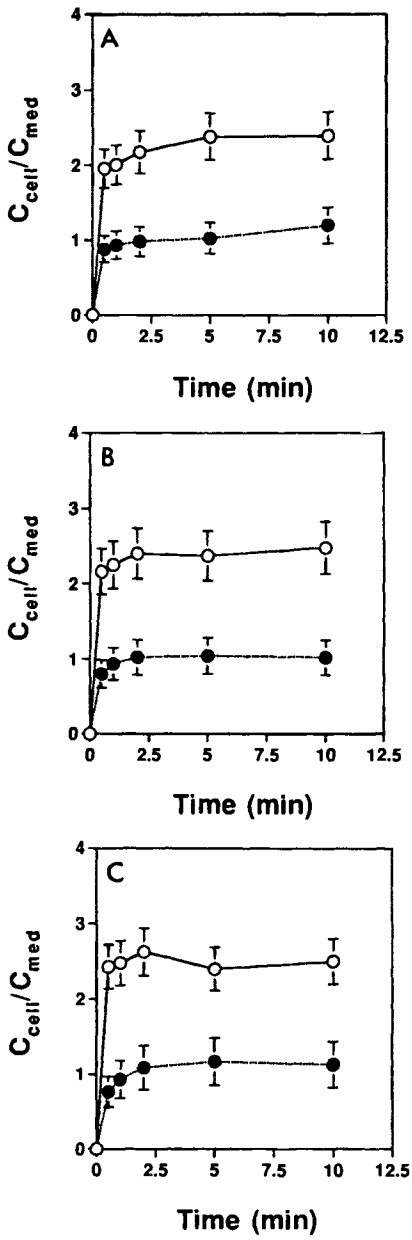

Fig. 7. Time-course of cell-to-medium concentration ratio for parent YM796 under conditions where no metabolism is assumed to occur. The unbound fraction of YM796 in hepatocytes was estimated from Eq. (11) at two concentrations of YM796 (5 and 1000 μM) under three different conditions where no metabolism was assumed to occur, i.e. in the presence of SKF-525A (500 μM) which is a typical inhibitor of P-450 (A), at low temperature (4°C) (B), and after treatment with carbon monoxide (CO) which also inhibits P-450 activity (C). ○, 5 μM; ●, 1000 μM.

that obtained in rat liver microsomes (38.8 ml/min/g liver) reported previously. Houston indicated the intrinsic metabolic clearances obtained in rat liver microsomes were lower than those obtained in isolated rat hepatocytes for various high-clearance drugs and also lower than the $CL_{int,in\ vivo}$ (14). In addition, it has been reported the K_m values for antipyrine and ethylmorphine obtained in liver microsomes were greater than those estimated using hepatocytes (15,16,17). As a reason for

this, it is often claimed the prepared liver microsomes do not represent physiological condition and the experimental conditions for metabolic studies could not always be optimized (14). Another reason worth considering is the possibility of underestimating the intrinsic metabolic clearance in liver microsomes because no correction is made for the unbound concentration of the drug in the incubation medium which may fall due to binding to microsomes (18). In the case of YM796, unlike these drugs, the intrinsic metabolic clearance for liver microsomes was slightly higher than that for hepatocytes. This is probably because CL_{int} was greater than PS_{eff} under linear conditions and $CL_{int,all}$ was affected by the membrane permeability clearance. Since the *in vivo* unbound plasma concentration of YM796 was lower than the minimum concentration used in the present study, for rats, it seemed unlikely that $CL_{int,in\ vitro}$ was equal to $CL_{int,in\ vivo}$. However, the intrinsic metabolic clearance for liver microsomes (38.8 ml/min/g liver) was only slightly greater than that for *in vivo* (30.4 ml/min/g liver) (2). Thus, it is probable the intrinsic metabolic clearance for liver microsomes may still be underestimated. Actually, in this study, the intrinsic metabolic clearance for the unbound YM796 in hepatocytes (CL_{int}/f_T) estimated from CL_{int} and f_T at the low concentration (5 μM) was 65.3 ml/min/g liver. The approximately 1.7-fold difference in the intrinsic metabolic clearance between microsomes and hepatocytes may be attributable to the interindividual differences, the difference in the experimental methods, and chances. In any case, the *in vivo* intrinsic metabolic clearance of YM796 seems closer to that for hepatocytes rather than that for microsomes.

On the other hand, the apparent amount of drug taken up by hepatocytes normalized by the initial YM796 concentrations in the medium ($X_t/C_{med}(0)$ [μl/mg protein]) fell as the concentration of YM796 increased (Fig. 4). At low concentrations (5 μM) of YM796, the proportion of metabolites to the total amount of drug in the cells was approximately 90% and fell at high concentrations (1000 μM) by up to approximately 50%, which was almost comparable with the intact drug. The proportion of metabolites to the total amount of drug in the medium was also markedly reduced, suggesting saturation of the hepatic metabolism of YM796 (Fig. 1). Since the proportion of the dose represented by intact YM796 in the cells did not differ greatly at 5 μM and 1000 μM, it was considered the reduction in $X_t/C_{med}(0)$ observed when the concentration of YM796 increased (Fig. 4) could be ascribed to a reduction in the metabolic trap caused by the reduced formation of metabolites which barely undergo any efflux from the liver. Actually, while the PS_{inf} values estimated based on Eq. (7) were almost constant (88 ~ 114 μl medium/min/mg protein) irrespective of the concentration of YM796, CL_{int} obtained from Eq. (8) fell markedly from 102 to 1.5 μl cellular space/min/mg protein, showing the saturation of hepatic metabolism as the concentration of YM796 increased (Fig. 5). On the other hand, PS_{eff} calculated from the aforementioned PS_{inf} and CL_{int} values based on Eq. (9) increased, unlike the CL_{int}, at higher concentrations of YM796 and reached a value almost similar to that of PS_{inf} at 100 ~ 1000 μM (Fig. 5). Bearing in mind the fact that PS_{eff} is the efflux clearance defined in terms of the total concentration of intact YM796 in the cells and the unbound fraction of YM796 in the liver increased from 0.41 to 0.90 when the concentration of YM796 increased from 5 to 1000 μM (Fig. 7), this increase in PS_{eff} may be attributed to an increase in the unbound fraction of YM796 in the liver resulting from the saturation of the tissue binding at higher concentrations of YM796. The increase in PS_{eff} seems greater than that in f_T when the concentration of YM796 in the medium increased (Figs. 5, 7). In other words, $PS_{u,eff}$ (defined in terms of the unbound concentration of drug in the liver) obtained from PS_{eff} by correcting for the tissue binding also has a tendency to increase with the increase in the drug concentration in the medium. There are two possible reasons for this apparent concentration-dependent increase in $PS_{u,eff}$; first, PS_{eff}, calculated by Eq. (9) using the multiple parameters and measured values, PS_{inf}, CL_{int}, $C_{cell,ss}$, and $C_{med,ss}$, may have some estimation error caused by the accumulation of each error, second, the assumption of a well-stirred condition from which Eq. (9) was derived may not be valid. In fact, for some drugs, the presence of a deep intracellular pool or the intracellular diffusion limited elimination has been reported (19,20,21).

$PS_{u,eff}$ is close to PS_{inf} at high concentrations of YM796 (1000 μM). In addition, since PS_{inf} was never more than twice as great as $PS_{u,eff}$ even at a low concentration (5 μM), and PS_{inf} was hardly affected by the concentration of YM796, the contribution of carrier-mediated active mechanism to the transport of YM796 through the sinusoidal membrane is considered to be low.

Furthermore, at low concentrations of YM796, $CL_{int,all}$ was close to PS_{inf}, then fell, as the concentration of YM796 increased and, finally, at high concentrations, became almost equal to CL_{int} (Figs. 3, 5). At low concentrations of YM796, CL_{int} was greater than PS_{eff} and $CL_{int,all}$ could be affected by membrane permeability while, at high concentrations, where saturation of YM796 metabolism occurred, CL_{int} fell and became much lower than PS_{eff}. In addition, f_T was close to unity and the contribution of carrier-mediated active transport was low. For these reasons, $CL_{int,all}$, at relatively high concentrations of YM796, apparently reflects the CL_{int} (intrinsic metabolic clearance-limited). Thus, the $K_{m,app}$ and V_{max} values obtained in the present study using isolated rat hepatocytes seems to be fairly consistent with those obtained in liver microsomes previously reported (2). Since the $CL_{int,in\ vitro}$ values for dogs and humans were, respectively, approximately 1/15 and 1/40 lower than for rats (1,2), the $CL_{int,all}$ for dogs and humans is considered to be much less affected by membrane permeability clearance than for rats.

In conclusion, $CL_{int,all}$ for YM796 estimated from rat hepatocytes was shown to be affected to some degree by the membrane permeability clearance at low concentrations since CL_{int} was greater than PS_{eff}, and became completely rate-limited by intrinsic metabolism at high concentrations of YM796 where CL_{int} fell due to saturation of metabolism.

REFERENCES

1. T. Iwatsubo, H. Suzuki, N. Shimada, K. Chiba, T. Ishizaki, C. E. Green, C. A. Tyson, T. Yokoi, T. Kamataki, and Y. Sugiyama. Prediction of *in vivo* hepatic metabolic clearance of YM796 from *in vitro* data using human liver microsomes and recombinant P-450 isozymes. *J. Pharmacol. Exp. Ther.* **282**:909–919 (1997).
2. T. Iwatsubo, H. Suzuki, and Y. Sugiyama. Prediction of species differences (rats, dogs, humans) in the *in vivo* metabolic clearance of YM796 by the liver from *in vitro* data. *J. Pharmacol. Exp. Ther.* **283**:462–469 (1997).

3. T. Iwatsubo, N. Hirota, T. Ooie, H. Suzuki, N. Shimada, K. Chiba, T. Ishizaki, C. E. Green, C. A. Tyson, and Y. Sugiyama. Prediction of *in vivo* drug metabolism in the human liver from *in vitro* metabolism data. *Pharmacol. Ther.* **73**:147–171 (1997).
4. K. Ito, T. Iwatsubo, S. Kanamitsu, Y. Nakajima, and Y. Sugiyama. Quantitative prediction of *in vivo* drug clearance and drug interactions from *in vitro* data on metabolism together with binding and transport. *Ann. Rev. Pharmacol. Toxicol.* **38**:461–499 (1998).
5. Y. Sugiyama, Y. Sawada, T. Iga, and M. Hanano. Xenobiotic metabolism and disposition. In R. Kato, R. W. Estabrook, and M. N. Cayen (eds.), *Proceedings of the 2nd international ISSX meeting*, Taylor & Francis, London, 1988, pp. 225–235.
6. S. Miyauchi, Y. Sawada, T. Iga, M. Hanano, and Y. Sugiyama. Comparison of the hepatic uptake clearances of fifteen drugs with a wide range of membrane permeabilities in isolated rat hepatocytes and perfused rat livers. *Pharm. Res.* **10**:434–440 (1993).
7. H. Baur, S. Kasperek, and E. Pfaff. Criteria of viability of isolated liver cells. *Heppe-Seyler's Z. Physiol. Chem.* **356**:827–838 (1975).
8. M. Schwenk. Transport systems of isolated hepatocytes. Studies on the transport of biliary compounds. *Arch. Toxicol.* **44**:113–126 (1980).
9. M. Yamazaki, H. Suzuki, Y. Sugiyama, T. Iga, and M. Hanano. Uptake of organic anions by isolated rat hepatocytes. A classification in terms of ATP-dependency. *J. Hepatol.* **14**:41–47 (1992).
10. K. Yamaoka, Y. Tanigawara, T. Nakagawa, and T. Uno. A pharmacokinetic analysis program (MULTI) for microcomputer. *J. Pharm. Dyn.* **4**:879–885 (1981).
11. S. Miyauchi, Y. Sawada, T. Iga, M. Hanano, and Y. Sugiyama. Dose-dependent hepatic handling of *l*-propranolol determined by multiple indicator dilution method: Influence of tissue binding of *l*-propranolol on its hepatic elimination. *Biol. Pharm. Bull.* **16**:1019–1024 (1993).
12. M. Yamazaki, S. Akiyama, R. Nishigaki, and Y. Sugiyama. Uptake is the rate-limiting step in the overall hepatic elimination of pravastatin at steady-state in rats. *Pharm. Res.* **13**:1559–1564 (1996).
13. R. N. Zahlten and F. W. Stratman. The isolation of hormone-sensitive rat hepatocytes by a modified enzymatic technique. *Archs. Biochem. Biophys.* **163**:600–608 (1974).
14. J. B. Houston. Utility of *in vitro* drug metabolism data in predicting *in vivo* metabolic clearance. *Biochem. Pharmacol.* **47**:1469–1479 (1994).
15. R. R. Erickson and J. L. Holtzman. Kinetic studies on the metabolism of ethylmorphine by isolated hepatocytes from adult rats. *Biochem. Pharmacol.* **25**:1501–1506 (1976).
16. A. Rane, G. R. Wilkinson, and D. G. Shand. Prediction of hepatic extraction ratio from *in vitro* measurement of intrinsic clearance. *J. Pharmacol. Exp. Ther.* **200**:420–424 (1977).
17. J. S. Hayes and K. Brendel. N-demethylation as an example of drug metabolism in isolated rat hepatocytes. *Biochem. Pharmacol.* **25**:1495–1500 (1976).
18. R. S. Obach. The importance of nonspecific binding in *in vitro* matrices, its impact on enzyme kinetic studies of drug metabolism reactions, and implications for *in vitro-in vivo* correlations. Drug Metab. Dispos. **24**:1047–1049 (1996).
19. K. Sathirakul, H. Suzuki, K. Yasuda, M. Hanano, O. Tagaya, T. Horie, and Y. Sugiyama. Kinetic analysis of hepatobiliary transport of organic anions in Eisai hyperbilirubinemic mutant rats. *J. Pharmacol. Exp. Ther.* **265**:1301–1312 (1993).
20. K. Sathirakul, H. Suzuki, K. Yasuda, M. Hanano, and Y. Sugiyama. Construction of a physiologically based pharmacokinetic model to describe the hepatobiliary excretion process of ligands: Quantitative estimation of intracellular diffusion. *Biol. Pharm. Bull.* **16**:273–279 (1993).
21. E. Tipping and B. Ketterer. The influence of soluble binding proteins on lipophile transport and metabolism in hepatocytes. *Biochem. J.* **195**:441–452 (1981).